Temporal Evolution of Polarization in M87 Insights from GRMHD Simulations

Joaquin Duran, Richard Anantua, Brandon Curd, Hayley West, & Lani Oramas
The University of Texas at San Antonio, San Antonio TX, 78249

Abstract

Our research delves into the intricate dynamics of M87, a key subject in astrophysics due to its extraordinary jet and supermassive black hole, recently imaged by the Event Horizon Telescope (EHT). This study aims to explore the temporal evolution of polarization within M87, utilizing GRMHD simulations to bridge the gap between theoretical predictions and EHT observations, thereby offering new insights into the mechanisms governing its jet and accretion dynamics.

Introduction

M87, an iconic supergiant elliptical galaxy featuring a significant jet powered by its central supermassive black hole (SMBH), has been a focal point in astrophysics, especially following the Event Horizon Telescope (EHT) capturing its black hole's shadow. The temporal evolution of polarization within M87's jet remains a pivotal, yet underexplored aspect crucial for unraveling the SMBH's accretion and jet ejection mechanisms. Addressing this gap, our study leverages advanced three-dimensional general relativistic magnetohydrodynamic (GRMHD) simulations to probe the polarization dynamics in M87. By aiming to align theoretical insights with empirical observations from EHT, specifically through the lens of median linear polarization during significant simulation intervals, our research endeavors to enhance the comprehensive understanding of the complex processes at play around supermassive black holes, thus bridging a vital gap in the astrophysical narrative on AGNs.

Methods

- General Relativistic Radiative Transfer (GRRT) Codes: IPOLE is used to ray-trace GRMHD simulations, allowing the simulation of polarimetric images of these simulations
- Functionality: It solves for the evolution of polarized intensities along a geodesic using a two-stage operator splitting method. This involves:
  - First Stage: Parallel transport of the covariant coherency tensor (related to invariant Stokes parameters and Pauli matrices) along the geodesic
  - Second Stage: Updating the Stokes parameters using an analytic solution to the explicit general polarized transport with constant emission, absorption, and rotation coefficients computed in the local orthonormal tetrad defined by the fluid and magnetic field.
- Image Production: IPOLE produces images comprising a square grid of pixels, each reporting Stokes intensities for I, Q, U, and V, over a specified field of view. This requires specifying physical scales such as mass-density of accreting plasma, size of the black hole, and the observer's orientation
- Adjustments for High Magnetization: GRMHD codes, including IPOLE, often introduce artificial mass and energy in regions of high magnetization due to the inability to accurately evolve the fluid state in these regions. This can lead to unphysically high plasma density and temperature in areas of large magnetization

Results

	. $R-\beta$	SANE $R-\beta$ w./ jet	$(a=-0.5)$ Critical β	Critical β w./ jet	$R-\beta$	MAD $R-\beta$ w./ jet	$(a=-0.5)$ Critical β	Critical β w./ jet
$\lvert m\rvert_{\rm net}(f_{\rm pos,\,min})$	5.00×10^{-3}	7.26×10^{-3}	3.46×10^{-3}	5.84×10^{-3}	4.92×10^{-2}	$\mathbf{2.90\times10^{-2}}$	4.77×10^{-2}	3.44×10^{-2}
$\lvert m\rvert_{\rm net}(f_{\rm pos,\,max})$	3.81×10^{-3}	6.56×10^{-3}	2.74×10^{-3}	6.14×10^{-3}	$\boldsymbol{3.71\times10^{-2}}$	$\mathbf{3.10\times10^{-2}}$	4.07×10^{-2}	$\mathbf{3.31\times10^{-2}}$
$<\lvert m\rvert>(f_{\rm pos,\,min})$	$\mathbf{9.43\times10^{-2}}$	$\mathbf{1.02\times10^{-1}}$	$\mathbf{6.17\times10^{-2}}$	$\mathbf{8.85\times10^{-2}}$	3.49×10^{-1}	3.30×10^{-1}	2.71×10^{-1}	2.61×10^{-1}
$<\lvert m\rvert>(f_{\rm pos,\,max})$	$\mathbf{9.49\times10^{-2}}$	1.08×10^{-1}	$\mathbf{6.55\times10^{-2}}$	$\mathbf{9.72\times10^{-2}}$	4.49×10^{-1}	4.31×10^{-1}	3.88×10^{-1}	3.91×10^{-1}

Table 8: Above shows median linear polarization for times 20,000M ≤ T ≤ 30,000M. Bold values mark SANE and MAD models with a/M = -0.5 meeting EHT M87's polarization constraints (0.01 ≤ |m|_net ≤ 0.037, 0.057 < |m| > < 0.107), highlighted in italics for models meeting these criteria

Table 9: Below presents median circular polarization for times 20,000M ≤ T ≤ 30,000M. Italic values denote SANE and MAD models with a/M = -0.5 that do not meet the constraints |v|_net ≤ 0.008 and < |v| > ≤ 0.037

	. $R-$Beta	SANE $R-$Beta w./ Jet	$(a=-0.5)$ Crit. Beta	Crit. Beta w./ Jet	$R-$Beta	MAD $R-$Beta w./ Jet	$(a=-0.5)$ Crit. Beta	Crit. Beta w./ Jet
$\lvert V\rvert_{\rm net}(f_{\rm pos,min})$	$-3.53\cdot10^{-3}$	$-2.26\cdot10^{-3}$	$-4.53\cdot10^{-3}$	$-1.42\cdot10^{-3}$	$-3.85\cdot10^{-3}$	$-2.61\cdot10^{-3}$	$-3.27\cdot10^{-3}$	$2.34\cdot10^{-3}$
$\lvert V\rvert_{\rm net}(f_{\rm pos,max})$	$-2.81\cdot10^{-3}$	$1.76\cdot10^{-3}$	$2.02\cdot10^{-3}$	$1.85\cdot10^{-3}$	$-3.14\cdot10^{-3}$	$-1.36\cdot10^{-3}$	$-3.19\cdot10^{-3}$	$-1.54\cdot10^{-3}$
$<\lvert V\rvert>(f_{\rm pos,min})$	$8.39\cdot10^{-3}$	$7.07\cdot10^{-3}$	$1.67\cdot10^{-2}$	$8.12\cdot10^{-3}$	$3.24\cdot10^{-3}$	$2.26\cdot10^{-3}$	$3.05\cdot10^{-3}$	$2.32\cdot10^{-3}$
$<\lvert V\rvert>(f_{\rm pos,max})$	$1.42\cdot10^{-2}$	$1.04\cdot10^{-2}$	$\boldsymbol{3.99\cdot10^{-2}}$	$1.86\cdot10^{-2}$	$1.23\cdot10^{-3}$	$6.11\cdot10^{-4}$	$1.17\cdot10^{-3}$	$6.75\cdot10^{-4}$

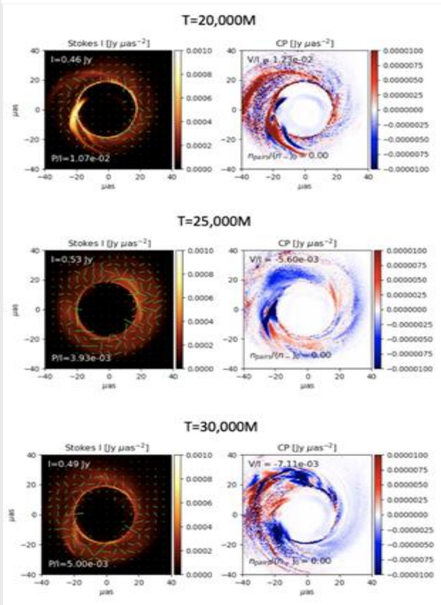

The figure to the left displays a time series for the a = -0.5 SANE model at T = 25,000M, featuring R – β at 230 GHz without positrons. It includes three panels: the top panel at T = 20,000M, the middle panel at T = 25,000M, and the bottom panel at T = 30,000M, offering a detailed look at the SANE model's evolution over time

The figure on the right showcases a time series for the a = -0.5 MAD model at T = 25,000M, illustrating R – β at 230 GHz without positrons. It presents three distinct panels: the top panel at T = 20,000M, the middle panel at T = 25,000M, and the bottom panel at T = 30,000M, providing a comprehensive view of the model's dynamics over time.

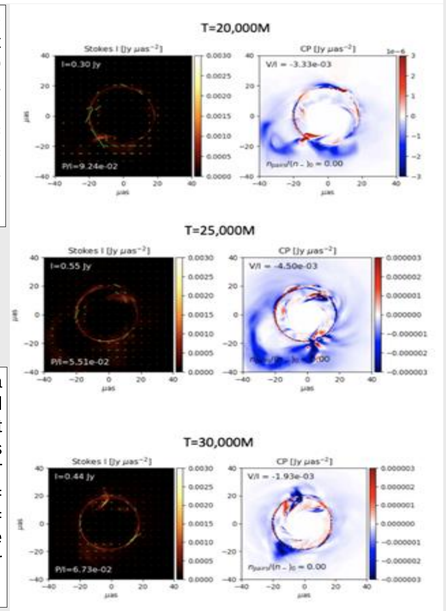

Conclusions

- Key Findings:
- Demonstrated that the temporal evolution of polarization in M87 can be systematically analyzed through 3D GRMHD simulations.
- Identified specific correlations between black hole spins, plasma compositions (SANE vs. MAD models), and observed polarization patterns, enriching our understanding of jet emission mechanisms.
- Provided evidence that both SANE and MAD models can meet the stringent polarization constraints observed in M87, highlighting the complexity of the accretion flow dynamics.

- Implications:
- Enhanced the predictive power of models concerning polarized emission in AGNs, offering insights into the underlying physics of jet formation and evolution.
- Established a framework for future observational campaigns to test simulation predictions, potentially refining our understanding of black hole physics.
- Contributed to the broader astrophysical discourse on the SANE/MAD dichotomy, promoting a deeper exploration of plasma dynamics near supermassive black holes.

Future Directions

- Refine Polarization Models: Advance SANE/MAD models to better predict polarization for various spins and plasmas.
- Enhance Observational Campaigns: Partner with EHT/VLBI for detailed polarization data, comparing it with simulations.
- Investigate Spin-Plasma Dynamics: Study black hole spin and plasma dynamics' impact on jet structure and polarization.
- Multi-Wavelength Observations: Expand research to include observations across different wavelengths for a fuller picture of M87.
- Compare with Other AGNs: Use findings to analyze other AGNs, aiming for a unified understanding of jetted AGN emission.

References

Anantua R., Ricarte A., Wong G., Emami R., Blandford R., Oramas L.,West H.,Duran J., et al., 2024, MNRAS, 528, 735. doi:10.1093/mnras/stad3998